Detection of Glaucoma Disease Using Machine Learning Techniques

Sandhya Bhattacharya[1]
Department of Computer Science & Engineering, Shri Shankaracharya Institute of Professional Management & Technology, Raipur, India
sandhya.bhattacharya@ssipmt.com

Yogesh Kumar Rathore[2]
Assistant Professor, Department of Computer Science & Engineering,
Shri Shankaracharya Institute of Professional Management & Technology, Raipur, India
y.rathore@ssipmt.com

*__Corresponding Author__: y.rathore@ssipmt.com

Article History: **Received:** 30.04.2023 **Revised:** 29.05.2023 **Accepted:**08.06.2023

Abstract: ***Glaucoma illness is growing increasingly common as a result of strain on the eye cells. Several image processing-based approaches have previously been employed to diagnose glaucoma, however their classification accuracy was lacking. Mobile phones and video games are increasingly being utilised in daily life, putting additional strain on the eye cells. In this study, the Bin Rushed database is utilised to illustrate three distinct ways for detecting glaucoma illness utilising image processing, machine learning, and a deep learning convolutional neural network model. Image processing techniques are used to extract features such as CDR and RDR, which are then classified using a neural network, support vector machine, and other approaches. The VVG-16 deep learning model has an accuracy of 99.6%, with the K nearest neighbour strategy having the highest accuracy of 98%.***

Keywords: Machine learning, Glaucoma, kernel, PYTHON, CNN, Rim-One, ConvNets

1. Introduction

Glaucoma is a complicated disease that damages optical nerve and causes irreversible blindness due to lack of proper diagnosis. This “sneak thief of sight” can affect anyone at any age. Even newborn babies can be affected. According to doctors, it grows in such a manner that patient does not experience any complication. By 2040, the number of glaucoma affected people likely to increase 111.8 million [2]. Glaucoma causes vision loss and blindness due to damage of optic nerve. Our optic nerve provides visual sensation to our brain from both eyes. We know, eyes continuously make aqueous humor and it fills the front part of eyes. If the drainage channels of aqueous humor are blocked, the IOP (Intraocular pressure) increases and optic nerve may become permanently damaged. There are five major types of glaucoma: Open angle glaucoma, Angle Closure Glaucoma, Congenital Glaucoma, Normal Tension Glaucoma and Secondary Glaucoma. For glaucoma diagnosis, ophthalmologist need to perform a comprehensive examination of eye, including Tonometry, Gonioscopy, Ophthalmoscopy, Nerve fiber analysis and Perimetry. These diagnosis procedures are expensive and also time consuming. So, to cope with this great ocular problem, a CNN architecture will be approached for glaucoma detection.

Glaucoma is one of the most dangerous causes of blindness. Sometimes patient have no symptoms and the vision may remain 6/6 till late stage. Actually, there are no specific symptoms during early stage. Some patient may never have increased Intra-ocular pressure. Besides some patient with high Intra-ocular pressure may not diagnose glaucoma, which is called ocular hyper tension. Early detection of glaucoma associated with immediate treatment that has been shown to prevent major problems.

Glaucoma is nothing but the multi factorial neurodegenerative disease, which is degrades the vision over time which is responsible for loss vision of 66.8 million people in all over the world. To evaluate the potential risk of the disease is take too much time in diagnose as well as for treatment of the glaucoma disease. Intra ocular pressure (IOP) is the elevated blood pressure within the eye, and as the disease progresses, it reaches a harmful amount, causing the optic nerve axon to split. As a result, the key risk factor for developing glaucoma is an increase in IOP pressure. This will hasten the loss of vision and eventually lead to blindness. Glaucoma is similar to intraocular hypertension, except it causes damage to the optic nerve. Since the optic nerve was damaged, the brain was unable to receive image

information from the light receptors. The physiologist's complaint is the degeneration of optic nerve cells, which affects both the optic nerve head and the visual area. Even though glaucoma damage is permanent, early diagnosis and medical care recommended by ophthalmologists may help reduce the likelihood of vision loss. The diameter of a glaucoma eye varies more than the diameter of a normal eye due to fluid pressure.

Glaucoma is a condition of the optic nerve that worsens over time. It usually occurs when fluid accumulates in the front ofour eyes. The fluid inside a normal eye has a pressure of 21mm Hg. If the fluid level in our eyes rises, the pressure in our eyes rises, causing damage to the optic nerves. The condition progresses rapidly and can result in vision loss in both eyes. Glaucoma-related blindness, on the other hand, can also be avoided with early detection and care. In the early stages of glaucoma, there are normally no signs, and the condition progresses within the eye.

2. Literature Review

The effects of exposure to noise and other occurrences on medical images are well-known. The main aim of preprocessing an image is to enhance quality, reduce noise, resize the image for the required size, and so on. Prior to segmentation, one should first conduct a set of procedures aimed at addressing problems of noise, poor lighting, and retinal structures that affect the processing of the image. Because nonuniform illumination has a propensity to enhance contrast, nonuniform illumination may be corrected by using adaptive histogram equalization [3]. Segmentation is a procedure in which a signal is divided into meaningful components. Before the signal is segmented, research has been done to examine the ways to single out a channel. It is customary to use the red and green channels in order to segment OD and OC because they are very clearly represented in those channels. Morales et al. [4] used principal component analysis (PCA) to correlate pixel values across three color bands in order to help eliminate the influence of blood vessels on segmentation of OD, the results of which are shown in an improved image of the vascular tree. The Canny edge identification is then used to increase the distinction between vessels and nonvessels. Rodrigues et al. [5] utilized multiscale filtering based on Hessian using a genetic algorithm to get their optimum segmentation parameters for blood vessels. In Bharkad's research, he filtered the blood vessels and increased the optical depth area by using an equiripple low pass FIR filter [6].

Preprocessed image features are superior to raw image features. In kidneys, blood arteries are common, making it difficult to split them. Noise reduction and artery separation preprocessing can help with segmentation.

The Hough transform was shown to be efficient in separating OD in the red channel, as demonstrated by Hagiwara et al. [7]. Vessel displacement was computed using the chessboard metric, and several values were generated that allowed the diagnosis of normal and glaucoma fundus pictures. A new method was created that analyzes the flow of blood vessels in the optic nerve in order to identify and diagnose glaucoma. Using an intensity threshold, Rathore et al. [8] were able to compute clinical parameters for the first time by splitting the OD and OC. Bharkad et al. [6] utilized corner thresholding and point contour joining to segment the OD. According to Pardha Saradhi Mittapalli and Ahmadi et al. [9], a region-based active contour model takes into consideration restrictions on shape as well as other variables. Also, a novel segmentation method for optic cupsis proposed based on structural and gray level properties. When separating OD levels, color and intensity data are included. This is done via the use of clustering, which uses the regional variations in the shade to assign a color to each separate section of the OC.

Shukla et al. [10] segregated optical density by minimizing the objective function for grouping pixels (OD). To segment the OC, thresholding is used using Otsu segmentation. Dey and Dey [11] utilized a randomized Hough transform in combination with a Canny edge detection technique to obtain optical contours in their research. To diagnose glaucoma, Gustian et al. [12] used a fully convolution network (FCN) and collected patient data and the contours of anatomical structure from case reports, and they were able to produce an image of the fundus. The authors of the work described in this paper used convolution neural networks to distinguish OC and OD pictures in their research, as Htay and Maung [13] reported. The filters provide data that is then sent to a softmax logistic classifier, which is a classifier that uses logistic regression.

Graph cut and convex hull procedures are used on the output of the classifier, which is segregated. In an effort to segment OD and OC pictures, Perdoma et al. built a deep neural network with 15 layers. The creation of a U-Net architecture was to help with the segmentation of OD and OC. This was done by Pandit et al. [14]. U-Net models have CNNs in them, and CNNs are the most vital part of a U-Net model. The latter of the two routes in this configuration grows, while the former shrinks.

The contracting route is implemented using the architecture of CNN with resolutionlayers that work well. The expansion layer resolution is verylow. The contracting path's image data is merged with the growing path's data. U-Net is able to identify patterns at a variety of scales.

Abbas [15] invented a hybrid strategy to identify the contours of OD and OC, which is also adaptively regularized and combines kernel-based fuzzy C-means (FCM) with the level set method to be able to differentiate between the two. Muthmainah et al. [16] invented a method for object classification utilizing super pixel classification, which classifies objects of interest (OD) and objects of concern (OC). Super pixel classification uses histogram features and sta- tistical data to find the disc's boundary and is where OD segmentation starts.

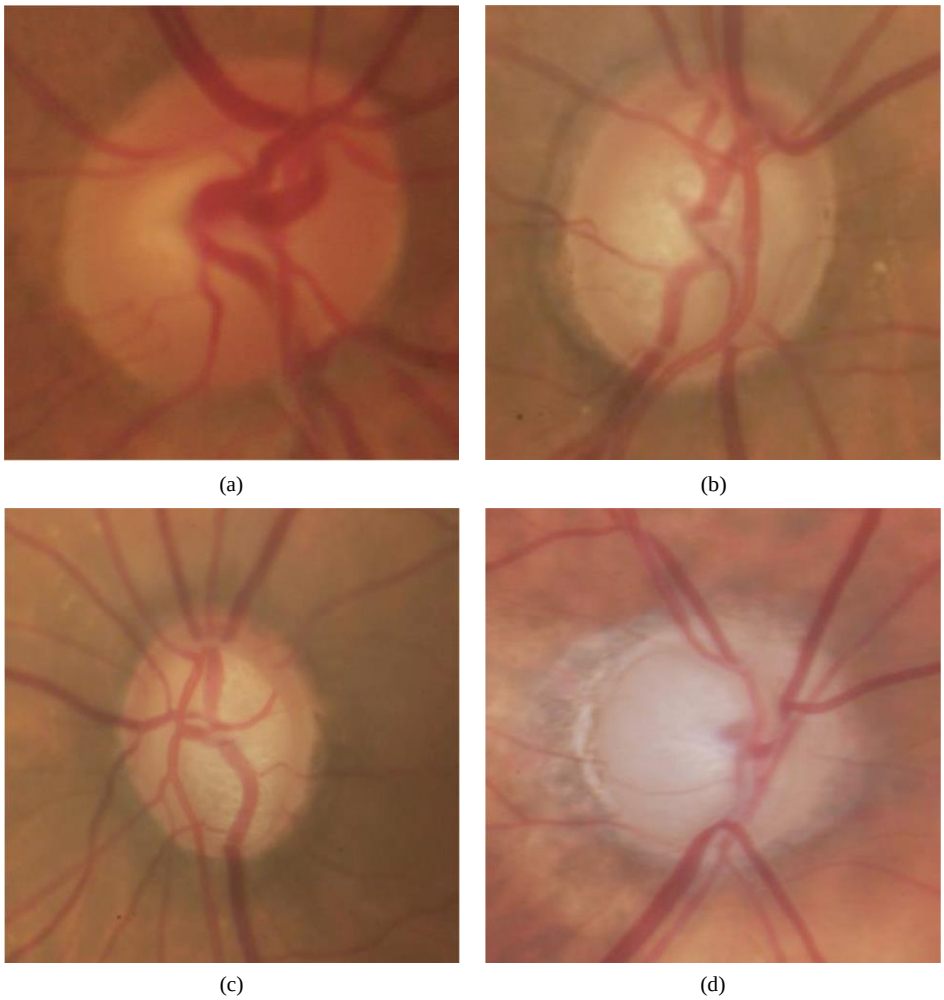

(a) (b)

(c) (d)

Fig 1: (a) Normal, (b) early glaucoma, (c) moderate glaucoma, and (d) severe glaucoma.

Fine-tuning is possible by using a deformable model. To get the most accurate segmentation, the algorithm relies on local knowledge. In a study conducted by Caroline et al., active contour model (ACM) was com- bined with gradient vector flow (GVF) Yu et al. [17] todeal with the standard snake's flaws, including an in- ability to move into concave parts of the image during advancement and a limited range of capture. The external energy in snake equations is replaced by the internal energy in GVF with the use of edge gradients. The circular Hough transform is used to determine the snake's out- line, the starting point of the analysis. After this, the snake is started with the OD boundary. In preparation for the snake's segmentation, GVF helps the snake regulate the OD boundary. A Hausdorff distance-based algorithm was used to locate the potential OD contours. Through the pyramidal decomposition method, it examines whether circular shapes may exist inside the different regions, just as a symbol might exist inside the OD. According to the study of Li et al. [18], an OD and OC segmentation contour-profiling model was developed to discover a category-based feature map optimization model that utilizes a region search to locate an optimal contour profile.

Muthmainah et al. [16] made progress in optical domain segmentation with the assistance of local binary patterns and density-based probability functions. To prevent segmentation mistakes, the red channel (which has a higher contrast) was segmented first, and all of the images were preprocessed with histogram equalization before being segmented. Pandit et al. [14] segmented the data for OD and OC by using a threshold technique. The author presents a multilevel thresholding approach for segmenting the image with fuzzy partitions of image histograms and entropy theory. In order to process the image, the RGB version of the picture is first converted into a grayscale version, and an image filtering technique is applied to reduce noise and enhance the results. The threshold for segmentation is determined using the Kapur test. Computing the CDR requires the use of the segmented OD and OC. The method for OD segmentation, as described by Tham et al. [19], involves the use of direction-based supervised learning between OD boundary coordinates, as well as a visual representation of OD, to show how it works. Kesarwani et al. [20] present a method for segmentation using a combination of CNN and dense-net methods. Convolutional blocks are densely connected together to form the pattern. The locally statistical ACM and a priori structure-based extraction is used to implement the model developed by Somogyi et al. [21] for OD and OC segmentation.

Hasan et al. present an article on end-to-end networks designed for segmentation and localization of OD and Foveacenters referred to as the DRNet. The method used was basedon circular area searching. However, to estimate the OD radius, the method requires information about the camera's range of view. Cheng et al. presented their study, which includes a multiscale method for segmenting OD and OC. Acreative CNN technique was used to create very dense feature maps, to get multiscale features. Features recovered by the pyramid filtering module via the pyramid filtering method. Bollwein and Westphal [22] proposed M-Net as a method for doing segmentation of OD and OC. The design of M-Net uses a multiscale input layer. To get a multilevel receptive field, an image pyramid is first created by down sampling images, which are then fed into the U-Net. The authors gave a multilevel loss to divide OD and OC based on the dice loss. Utama et al. [23] used a previously reported combination of RCNN to partition the OD and OC. Feature extraction begins with the VGG16 algorithm. Re- covery of missing features and the subsequent split of the signal into the disc network and the cup network is per- formed by sending information via two divergent, parallel branches. In order to figure out where the OC should be placed, the system employs a disc attention module to parsethe outcomes of the disc network and the cup network.

OC is hard to attain because of poor contrast, discontinuity of edges, and difficult-to-see OC and OD borders. A large number of techniques have similar effects on images with low contrast; they create under- and over segmentation. Thresholding-based methods are more accurate than other methods to segment retinal images. Despite the potential to improve OD and OC segmentation, deformed models are adversely affected by bright exudates at the OD border and will likely fail to segment the fundus image because of theirfailure to adequately capture OD and OC segmentation.Based on the learning provided by CNN-based methods, the most accurate characteristics learned from the training data are then used to evaluate the test data. They require a large data set to train a CNN. Changing the demarcation of the OD and OC components has a huge effect on the CDR and NRR properties. A good way to fulfill this expectation is to invent a new kind of segmentation.

An artificial neural network for machine learning is a supervised classification system that may be distributed simultaneously and includes input and output components that are linked together through a weighted connection. The weights are modified to match the input samples in order to better forecast the class, according to results from research performed by David et al. Instance classifiers are also known as KNN algorithms. For a vote-based categorization, testing data is placed into several categories, which include but are not limited to location and other criteria.

Yu et al. [17] proposed a technique that relies on the Na¨ıve Bayes theorem is used to classify exudates. Pixel-level descriptions are retrieved for each possible exudate region. Several new features were extracted from each pixel, and some of them were normalized with the average brightness of the optic disc in order to improve accuracy. Adaptive boosting is used to optimize Na¨ıve Bayes classifiers for pixel classification.

A limited number of reports have surfaced that describethe use of deep learning algorithms, such as CNN, for objectclassification. Convolution, pooling, and dense connection are three steps of a network that use convolution. At the convolution and pooling layer, the feature extraction pro- cedure reduces the sample dimensions.

In [24], how deep convolutional neural networks can beused to detect glaucoma in large screening campaigns using color fundus images is explored. The five architectures in- cluding standard CNN, VGG19, ResNet50, DENet, andGoogleNet performed well in terms of AUC, sensitivity, andspecificity.

Tham et al. [19] presented a deep learning-based computer-aided diagnosis system for the detection of glaucomatous optic neuropathy (GON) on color fundus photographs.

It is possible that many distinct classifiers may make a range of errors on several samples. The model's constraints also include the requirement for large training data sets [25]as the number of layers in the CNN rises [26]. These problems may cause network settings to be improperly configured because of network degradation and issues such as missing information [27]. Using dynamic classifier selection techniques, an ensemble of classifiers may be generated to accommodate any misclassifications [28].

Based on the inference drawn from the literature, the research gaps identified are as follows:

(i) There is a lack of an effective preprocessing approach for accurate segmentation

(ii) There is a lack of automated OD and OC segmentation techniques that overcome under- or over-segmentation due to the presence of exudates and low contrast between the boundaries

As part of the proposed work, fundus images will be used to identify anatomical structures along with pathological structures, and disease severity will be graded based on decision support tools to assist ophthalmologists.

Problem Statement

To design and implement glaucoma detection to find whether patients are suffering from eye disease.

3. Methodology

A. System Design

The methodology of this task is divided into three stages: pre-processing, run of GA which involves finding the simplest CNN architecture and run glaucoma classification of CNN. The proposed method's steps are represented in Figure 2(a).

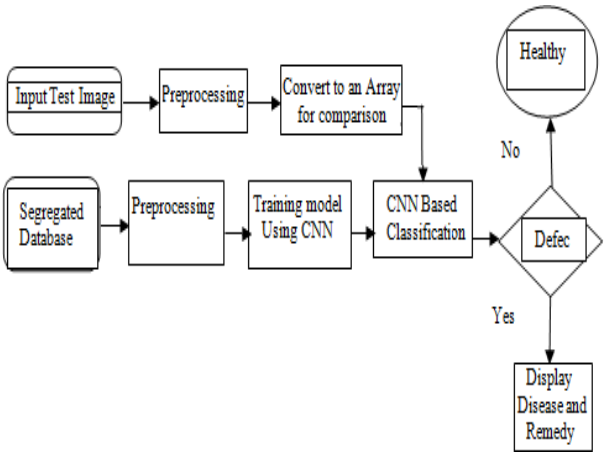

Figure 2(a): Machine Learning Model

B. System Architecture

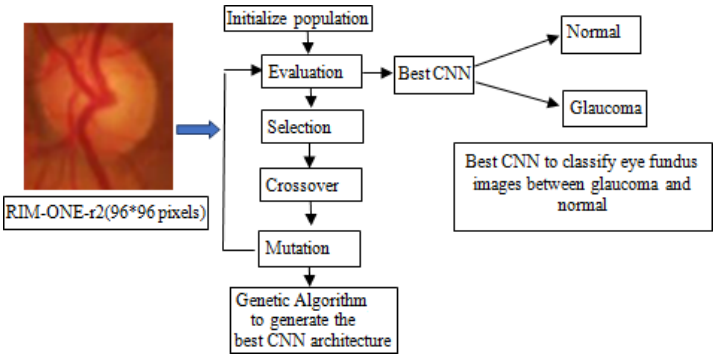

Figure 2(b): System Architecture

Rim-One, which was used in this research, is a public database that contains images of the I fundus in RGB (Red, Green, and Blue) format, as well as a guide for the creation of the optic nerve segmentation algorithm. In our experiments, we used version r2 of the Rim- One dataset, which includes images from the "glaucoma and suspect" class as well as images from the "standard" class. There are 455 images in the dataset, with 255 in the regular class and 200 in the "glaucoma and suspected" class. Pre-processing RIM-ONE-r2 with varying widths and heights yielded the images. The unique pre-processing technique used in this work is designed to fill the size of all images up to 96x96 pixels with a black pixel, with a technique known as zero-padding, with input pixels of input volume. Including zeroing the edge the format of images is thus beneficial for an accurate classification. A value of 96x96pixels was obtained from experience with poor results for another size (28x28, 32x32, 64x64 pixels). More than 96x96 pixels were also tested, but our GPU (Nvidia GeForceGTX 1060) memory could not support tests that supported output out memory errors. The entire image given by the RIM-One dataset was used as the input ROI (region of interest) for our method in this version of the dataset. This approach considered all information beyond the internal contents of the OD, such as the excavation, macula, and blood vessels. Genetic algorithms and training this work uses an approach to the development of automated CNN architectures. It is based on a neuro evolution technique known as NEAT (Neuro evolution of Augmenting Topology). The NEAT technique performs the optimization of components, topology and hyper parameters. The effect of the developed network is determined by how well they can be trained through gradient descent to perform the functionof classification. The genetic algorithm is a vampirism driven by the process of natural selection. It was proposed by John Holland (1975) and commonly used to generate high- quality solutions to optimization and discovery problems by relying on bio-inspired operators such as mutations, crossovers, and selection is done.

GA was evaluated by training each CNN generated on the same dataset partition: train data with 227 images, validationdata with 92 images, testing data with 136 images. Furthermore, this phase

lasted more than 200 epochs, using abath size of 16. The adapter function was used as an optimizer to compile each model and binary cross-entropy was used for loss, as our problem is a binary classification problem. To facilitate development and accelerate implementation, all processes were performed in Python with the Cairns API to initialize our GA, an initial population with 20 individuals is randomly created. This population should have 50% of batch normalization, determination, relay activation and dropout occurring with at least one layer (likely to be of other layers). Each individual (chromosome) is formed in a series of letters representing a specific layer, as described in Table 1 Example of a chromosome. B: batch normalization; C: determination; R: relay activation; d: dropout bcrd the evaluation function determines the fitness of an individual Due to our proposed concerns over resolving image classification tasks, classification verification loss is the best strategy to assign to their fitness (fitness=1/3loss). In this scenario, after training for this individual run with a slight validity loss, the best person from each generation will be chosen. Using the tournament selection criterion, the selection will return a random new parent, with the top performer being carried on to the next generation and mating with the rest of the population. Each child in the new population has a choice. Crossover is the technique that will choose a person's parents to mingle and merge their chromosomes to produce two new children. In our case, the parent layers must have the same length as the crossover occurs in the single point model and this point is chosen randomly, respecting the structural of the CNN. The probability of crossover in our GA is 30%. Utation, according to allow the algorithm to diversify populations, expanding the opportunity to search for unexplained regions in the search space for fitter solutions. The mutation is implemented by giving each element in the chromosome array randomly drawn the possibility of the following scenarios: deleting or adding determination clauses; Add or remove dropouts; Changing the order of punishment blocks; Changing the inputs of punishment blocks; Changing the output of large blocks; Change the order of large blocks. To evaluate each CNN, the training procedure was used on the train set data, the validation set data on the test set data of the RIM-ONE-R2, and the validated procedure on the test procedure.

4. Result analysis

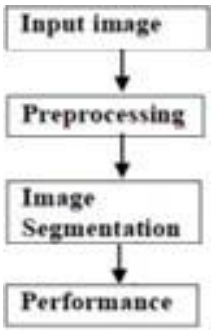

Figure 3: Flow chart

- The input test image is acquired and preprocessed in the next stage and it is converted into array form for comparison.
- The selected database is properly preprocessed and the renamed into proper folders.
- Though hemorrhage is difficult to detect, preprocessing is required to obtain a noise-free, clear, contrast-enhanced picture.

The steps including preprocessing to detect hemorrhages are:

a) Resize the image into 512*512 pixels.
b) Convert the RGB image into grey scale image.
c) Use Median Filtering to remove artifacts.
d) Equalize the image and enhance contrast.

- The model is properly trained using CNN then classification taker places.
- The comparison of the test image and trained model take place followed by the display of the result.

We begin by extracting the green channel from the image because the affected region is visible and easy to identify during this channel. Then we add a median filter with an 8-pixel radius to create a backdrop and subtract it from the original image. This results in a blood vessel and hemorrhage picture. We detach the vessel that ends during a picture with hemorrhages suggested using a vessel mask.

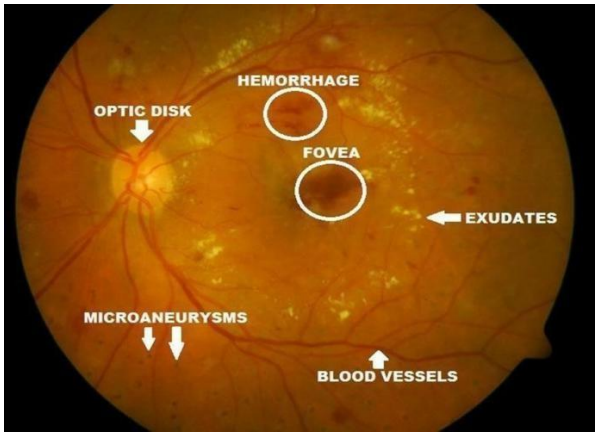

Figure 4: Retina with hemorrhages and exudates

A. Exudates detection

The method we have applied to detect exudates on human retina is inspired by the work described in [20]. Since the data set is of completely different characteristic as we've changed in various sides. That's why we are visiting describeevery step and so the rationale behind taking it. Here we wish to mention that we have got implemented some library provided by [21]. we've also used PYTHON version 2017a for this project and this detection consists of the next steps:

- Pre-processing the image.
- Detection of point and other artifacts.
- Detection of exudates in terms of optic disc and artifacts.

First, we extract intensity constituents from an image in the preprocessing phase. Here we are visiting work with gray-scale images because exudates are mostly visible in such images. We then apply Median Filtering for reducing the noise and apply Histogram Equalization to spice up contrast and brightness. The resulting image helps us to detect blind spot and accordingly exudates. This works as input image. Exudates are high intensity values likewise as optic disk. Therefore on travel for exudates detection we would like to go looking out blind spot then we'd prefer to differentiate between optic disc and exudates near and inside the blind spot area. To do and do that we consider that time is that the most important and most circular part in brightest portion of the image. We apply Gray Scale Closing is used to extract blood vessels from the retina, particularly in the blind spot region. We'll use a flat disc-shaped structure feature with an eight-radius radius. We binaries the image by thresholding it and using the resulting image as a mask. The mask is then inverted by pixels before being overlaid on the original image. On the overlaid image, we then apply reconstruction by dilation. We threshold the image and use the algorithm to find the difference between the original image and the reconstructed image. As a result, a high-intensity point is identified, and rests are eliminated.

In this section, we dealt with an infinite problem with this approach. The grey Scale Closing was used to delete vessels at the start of the strategy, and reconstruction was applied to the image produced from the initial image. As a result, we'll be visiting the aim area to reconstruct vessels. However, we have a problem in that there does not seem to be a single large circular blind spot. Rather, during this stage, we are detecting two or three large connected components. We used an addition dilation of the last word mask to solve this problem. As a consequence, the separate areas are bound in acircular pattern. We can see that there are already objects and other bright spots in the shot. As a consequence, if we use too much dilation, the blind spot can merge with those areas. A flat disc shaped structured feature with a radius of 4 was considered for the necessary additional dilation. Since the optic disc and also some bright artifacts are detected during this process, we've estimated for every component of the mask so on tell apart between the features some extra values. These additional values are termed as scores. Thuswe have, Score = area circularity 3.

Here's a situation that warrants your attention. We decided to give circularity more significance because we have a situation where the feature rather than the point can become much larger than the blind spot. We treat elements with a scale of less than 1100 pixels as a blind spot and treat therest as artefacts. Tiny areas that may become exudates are not classified as objects in this case. After point extraction and artefact detection, we'll look for exudates at this level. Grey Scale Closing, as before, eliminates high-intensity blood vessels. Then we decide to create a regular deviation picture that depicts the most important features of nearly organized exudates. Grey Scale Closing, as before, eliminates high-intensity blood vessels. Then we decide to create a regular deviation picture that depicts the most important features of nearly organized exudates. By setting the radius to six, the resulting image is thresholded. The surface outline of the retina is then removed, and the gaps are filled with imfill (). Threshold is used to exclude blind spots and objects. Finally, the result is obtained by applying an A level 0.01 threshold between the primary and thus the reconstructed data. To encourage accurate vision, the created exudates mask image is overlaid onto the primary image.

Figure 5 : Exudates detection. (a) Original image

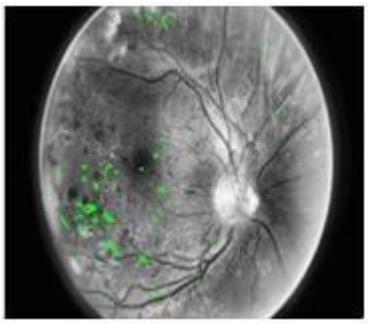

Figure 6: Exudates detection. (b) Exudates

After the entire feature extraction has been done, now we are visiting perform binary classification. Here we've used deep neural nets with two input layers, a whole of three layers, one representing the output. For this we've created a feed- forward back propagation network (newff). The phrases „newfit' and „newpr' stand for „regression' and „classification,' respectively. They together are called „newff" the generic name which continues to be available and provides better output in our classification.

First and foremost, we have built a two-stage feed forward network. Three „transit' neurons make up the first layer, andone „purelin' neuron makes up the second layer. As a result,we have

net = newff (p,t,[3,1],);

Here, p denotes the input vectors matrix and t denotes the goal vectors matrix. We used three components for the input vectors: blind spot mask, objects mask, and exudates mask.

The network is then simulated, and the results are plotted. As a result, we have y = sim(net, p);

We should notice that the network has been trained for 5000 epochs and the train-parameter target is 0.01. After the training is completed, a .mat file is created and loaded to test our datasets. If loaded, we can tell the difference between an

honest and a bad picture. Then the corr2 library function is used to hunt out the correlationbetween four classes of mages. The test image belongs to the category with which it correlates most.

Steps:

1) The input test image is acquired and pre-processed within the subsequent stage so it's converted into array form for comparison.
2) The selected database is correctly segregated and pre-processed so renamed into proper folders.
3) The model is correctly trained using CNN, Vgg16 Module then classification takes place.
4) The comparison of the test image and thus trained model occur followed by the display of the result.
5) If there is a retinal fundus it'll be classified.

B. Convolutional Neural Networks

The invention of the CNN in 1994 by Yann LeCun is what propelled the world of applied science and Deep learning to its former glory. The first neural network named LeNet5 had a awfully less validation accuracy of 42% since then we have got come a protracted way during this field. Nowadays almost every giant technology firms rely on CNN for more efficient performance. The concept to detect diseases in mulberry leaf incorporates the use of CNN before we dive into the "functionality and dealing of CNN" concept, we must have a basic idea on how the human brain recognizesan object in spite of its varying attributes from one another. Our brain features a fancy layer of neurons ,each layer holds some information about the article and each one the features of the article are extracted by the neurons and stored in our memory, next time after we see the identical object the brain matches the stored features to acknowledge the article, but one can easily mistake it as a simple "IF-THEN" function, yes it's to some extent but it's a further feature that has it a foot hold over other algorithms that's Self-Learning, although it cannot match a human brain but still it can provides it a difficult competition. Image is processed using the elemental CNN to detect the diseases in leaves. The data training in our CNN model must satisfy following constraints:

1) There should be no missing values in our dataset.
2) The dataset must distinctly be divided into training and testing sets, either the training or the testing set shouldn‟t contain any irrelevant data out of our model domain just in case of an image dataset all the pictures must be of the identical size, one uneven distribution of image size in our dataset can decrease the efficiency of our neural network.
3) The pictures should be converted into black and white format before feeding it into the convolution layer because reading images in RGB would involve a 3-D numPy matrix which might reduce the execution time of our model by a considerable amount.
4) Any quite corrupted or blurred images should even be trimmed from the database before feeding it into the neural network. Now we've learned the data pre-processing rules, allow us to dive right into the working of the convolutional neural network.

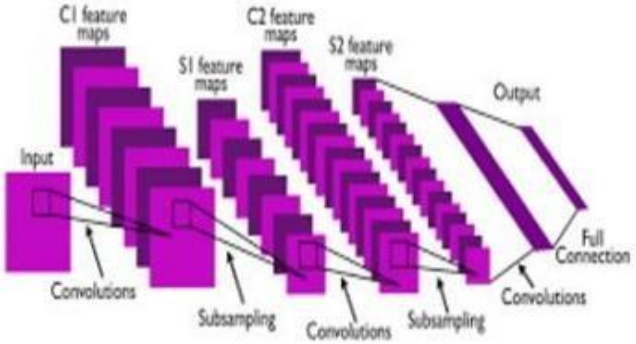

Figure 7: CNN layers

a) Convolution Layer

The pattern is identified by scanning the entire image and preparing it as a 3x3 matrix in this layer. The matrix kernel refers to the image's decorated function. A weight vector represents each value in the kernel.

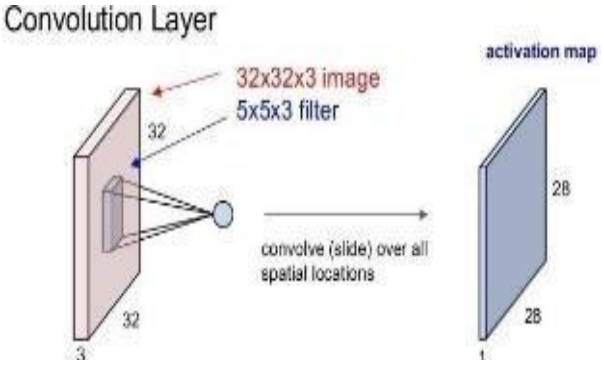

Figure 8 : Convolution Layer

b) Pooling layer

When it comes to pooling, the picture matrix breaks down into a collection of four non-overlapping rectangular segments. Pooling can be divided into two types: maximum pooling and average pooling. The maximum value in the relative matrix region that is taken is given to max pooling. The average value in the relative matrix region is obtained by average pooling. The pooling layer's key benefit is that it boosts device efficiency while reducing over-fittingopportunities.

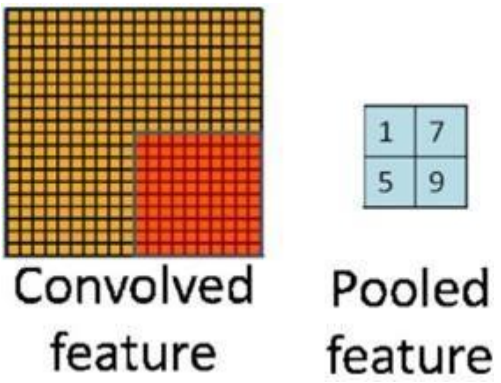

Figure 9: Pooling Layer

A. Activation layer

It is that part of the conversational neural networks where the values are normalized, fitting them within a certain range.

The determination used is ReLU which allows only positive values and then rejects negative values. It is a function of low computational cost.

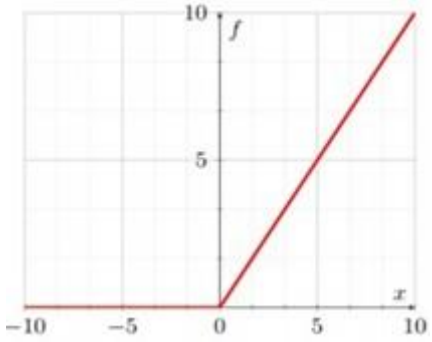

Figure 10: ReLU function

B. Fully joined layer

The features are compared to the test image's features, and the same features are applied with the defined mark. Labels are usually encoded as numbers for numerical convenience; they will be translated to their respective strings later.

Artificial intelligence has made significant progress in bridging the difference between human and computer capabilities. Researchers and enthusiasts alike work on a number of facets of the world in order to produce amazing items. The field of computer vision is one of these. The agenda for this field is to permit machines to work out the world as humans see it, to perceive it during a uniform way, and even to use knowledge foramess of tasks like image and video recognition, image analysis and classification, media recreation. recommendation systems, tongue processing, etc. Advances in deep learning computer vision are built and refined over time, primarily through a specific algorithm, a convolutional neural network.

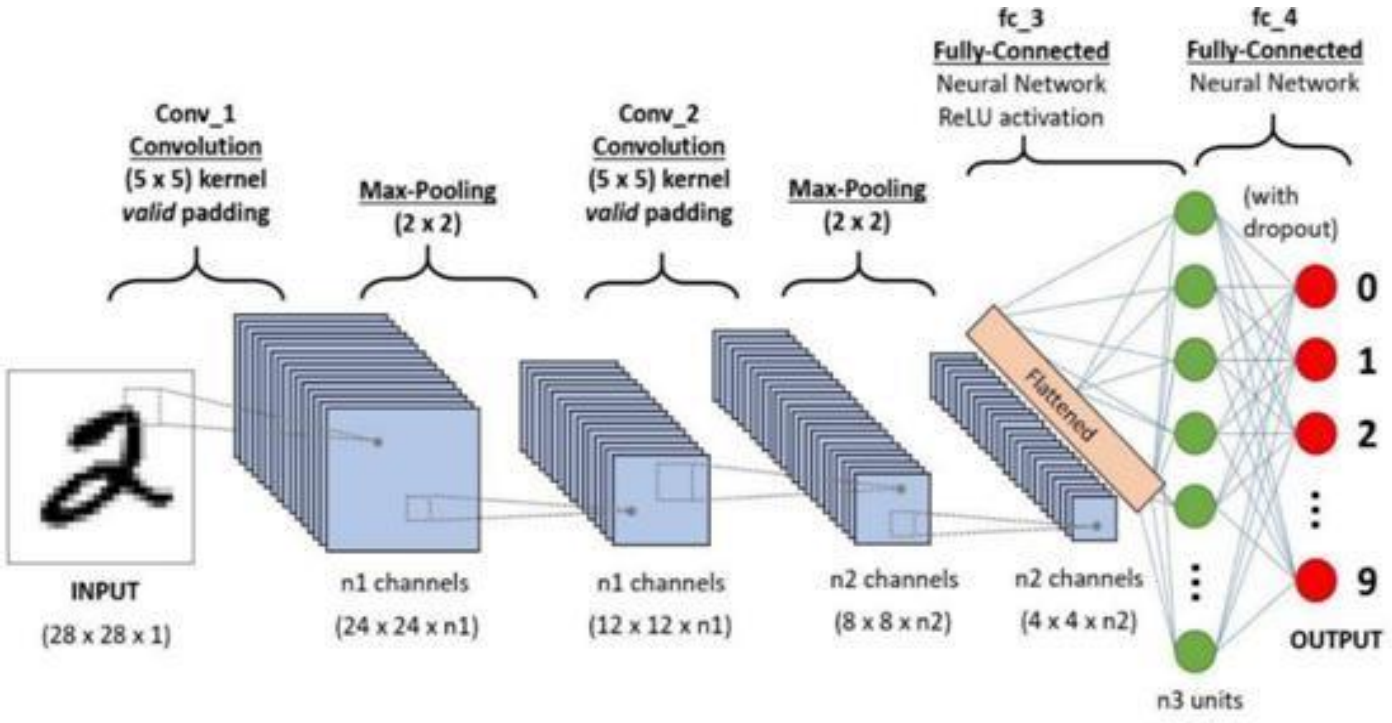

Fig 11: Activation layer

Input Image
4x4x3 RGB Image

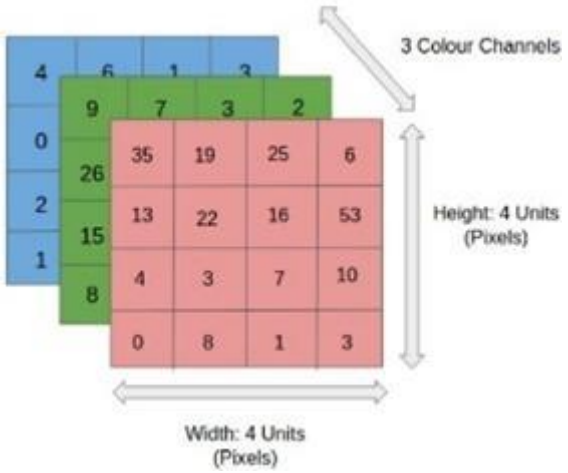

Fig 12 : RGB image

In the figure, we have an RGB image separated by three color planes-red, green and blue. There are several such color spaces in which images exist: grayscale, RGB, HSV, CMYK, etc.

You can imagine how computing resources will turn out when the images reach sizes, say, 8K (7680×4320). ConvNet's role is to transform images into a form that is easier to process without losing the functions that are critical to getting a good forecast. This is important when we want to design an architecture that is not only good at learning, but also scalable for massive datasets.

Convolution Layer the Kernel
Conversion of 5x5x1 image with a 3x3x1 kernel to request a 3x3x1 decorated feature Image dimensions = 5 (height) x 5 (width) x 1 (number of channels, eg. RGB)

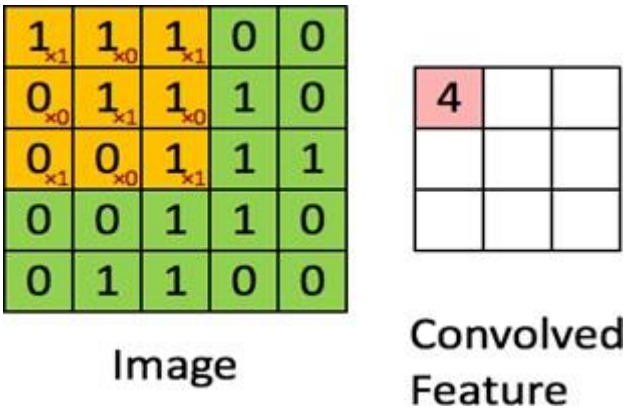

Fig 13: Convolution Layer the Kernel

In the above demonstration, the green segment corresponds to our 5x5x1 input image, I. The first element involved in completing the convolution operation within a part of a conventional layer named the kernel / filter, represented within the color yellow has gone. We have chosen K as the 3x3x1 matrix.

Kernel/Filter, K=

1 0 1
0 1 0
1 0 1

The core shifts 9 times due to the step length=1 (without sharpness), each time performing the matrix multiplication operation between K and part P of the image over which the core hangs.

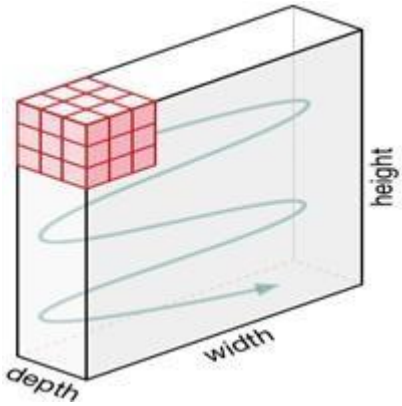

Fig 14 : Kernel Box

Kernel movement
The filter moves to the right with a fixed stride value until it crosses the entire width. Moving forward, it moves down to the beginning (left) of the image with the same stride

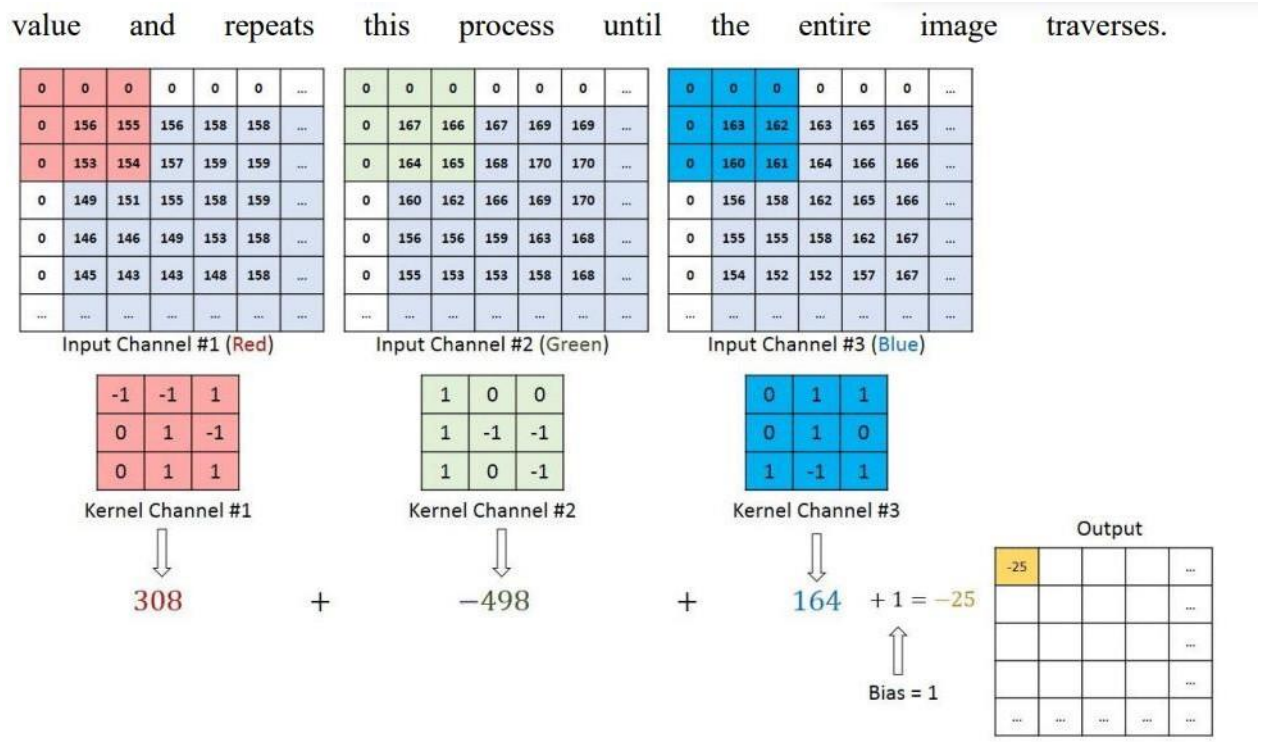

Fig 15 Convention operation on MxNx3 image matrix with 3x3x3 kernel

The kernel has the same depth as the input image in the case of images with multiple channels (such as RGB). Matrix multiplication is performed between the knee and the stack ([K1, I1]; [K2, I2]; [K3, I3]) and all results are expressed with bias such that the squash-depth channel's function performance is obtained.

The convention operation is used to detach high-level curvets from the input image as edges. There is no need to restrict Convent's to only one Convolutional Layer. The first converter is usually in charge of capturing low-level features like edges, color, gradient orientation, and so on. The design adopts high-level features with additional layers, giving us a network that makes sense. Similar representations of how we'd be in a dataset. There are two types of results of the operation - one in which the deflected attribute is reduced in dimensionality compared to the input, and the other in which the dimensionality is either increased or the same. This is done by applying a valid padding in the former case, or single padding in the latter case

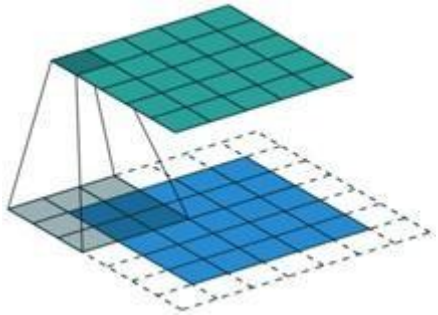

Fig 16: Padding

Same Filling: 5x5x1 image is supplemented with 0 s to create a 6x6x1 image

The convoluted matrix is 5x5x1 in size when we expand the 5x5x1 image to a 6x6x1 image and then add the 3x3x1 core to it. As a result, the gasket has the same name. On the other hand, if we perform the same operation without filling, we get a matrix that has the dimensions of the core (3x3x1) Valid Padding.

C. Results

Table 1 Performance of various model

Model	Test accuracy	Class name	Precision	Recall	F1 Score
InceptionResNet V3	**0.8526**	**Glaucoma** **Normal**	**0.86** **0.85**	**0.85** **0.86**	**0.85** **0.86**
DenseNet 121	**0.8153**	**Glaucoma** **Normal**	**0.74** **0.95**	**0.96** **0.68**	**0.84** **0.79**
ResNet50	**0.7761**	**Glaucoma** **Normal**	**0.83** **0.74**	**0.68** **0.87**	**0.75** **0.80**

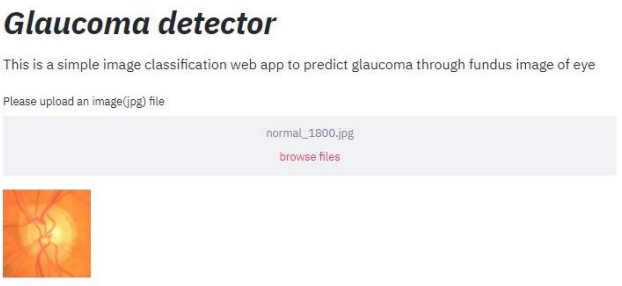

Fig 17: GUI of Proposed system when glaucoma detected

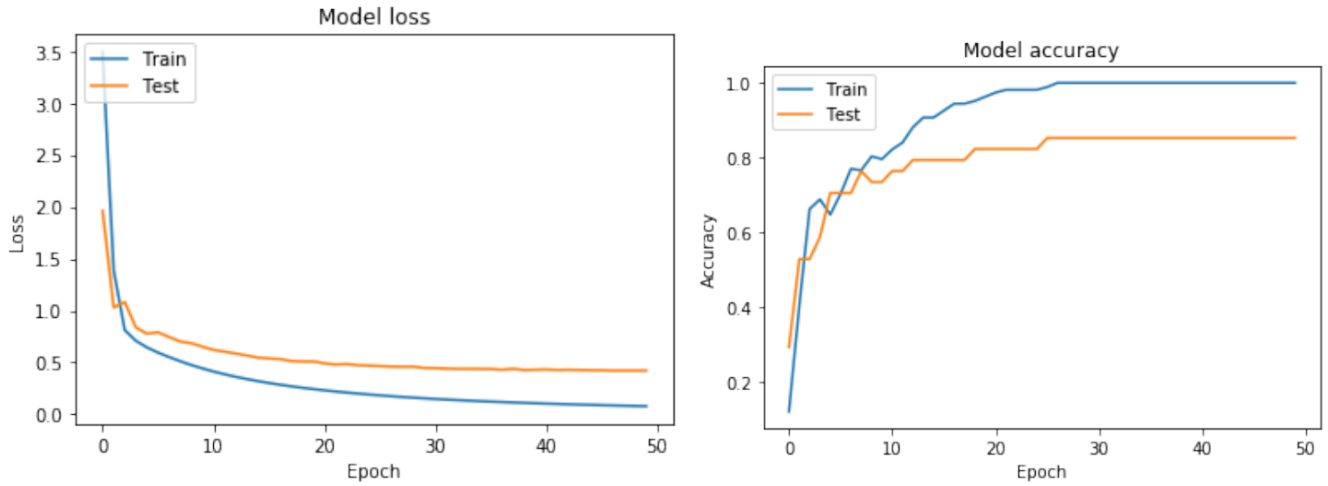

Figure 18: Accuracy detection

D. Conclusion

In this proposed work, an ensemble model was designed forthe detection of glaucoma in the early stage. In order to distinguish between normal and glaucomatous fundus pictures, the ensemble model proposes using a convolutionalneural network to extract feature information from the images. The performance of the proposed method of ensemble architecture is compared with three ConvNet architectures such as ResNet-50, VGGNet-16, and GoogLeNet. The proposed approach is tested on various public and private data sets.

The performance of the proposed algorithm is better than the state-of-the-art technique. The proposed ensemble model yields an accuracy of 91.13%, sensitivity of 86.58%, and specificity of 95.21% using PSGIMSR data set; accuracy of 98.67%, sensitivity of 100%, and specificity of 97.40% using HRF data set. Experiments conducted onboth public and private data sets show that the proposed model outperforms traditional computer-aided diagnosis algorithms and the convolutional neural network architecture. In this next proposed work, the investigation is carried out to design a fully convoluted network that can segment optic disc and optic cup with a large experimental data set.

References

[1] F. Guo, W. Li, J. Tang, B. Zou, and Z. Fan, "Automated glaucoma screening method based on image segmentation and feature extraction," *Medical, & Biological Engineering & Computing*, vol. 10, 2020.

[2] A. S. Derea, H. K. Abbas, H. J. Mohamad, and A. A. Al-Zuky, "Adopting run length features to detect and recognize brain tumor in magnetic resonance images," in *Proceedings of the 2019 First International Conference of Computer and Applied Sciences (CAS)*, pp. 186–192, Baghdad, Iraq, 18-19 Dec. 2019.

[3] F. Abdullah, R. Imtiaz, H. A. Madni et al., "A review on matic detection of optic disc based on PCA and mathematical morphology," *IEEE Transactions on Medical Imaging*, vol. 32, no. 4, pp. 786–796, 2013.

[4] S. Morales, V. Naranjo, J. Angulo, and M. Alcaniz, "Automatic detection of optic disc based on PCA and mathematical morphology," *IEEE Transactions on Medical Imaging*, vol. 32, no. 4, pp. 786–796, 2013.

[5] L. C. Rodrigues and M. Marengoni, "Segmentation of optic disc and blood vessels in retinal images using wavelets, mathematical morphology and Hessian-based multi-scale filtering," *Biomedical Signal Processing and Control*, vol. 36, pp. 39–49, 2017.

[6] S. D. Bharkad, "Frequency domain analysis of grey level intensities for extraction of optic disc in retinal images," *International Journal of Medical Engineering and Informatics*, vol. 13, no. 4, pp. 297–307, 2021.

[7] Y. Hagiwara, J. E. W. Koh, J. H. Tan, S. V. Bhandary, A. Laude, and E. J. Ciaccio, "Computer-aided diagnosis of glaucoma using fundus images: a review," *Computer Methods and Programs in Biomedicine*, vol. 165, pp. 1–12, 2018.

[8] N. Rathore, N. K. Jain, P. K. Shukla, and U. Rawat, "Image forgery detection using singular value decomposition with some attacks," *National Academy Science Letters*, vol. 44, pp. 331–338, 2021, https://doi.org/10.1007/s40009-020-00998-wUC.2021010102.

[9] N. Ahmadi and G. Akbarizadeh, "Iris tissue recognition based on GLDM feature extraction and hybrid MLPNN-ICA classifier," *Neural Computing & Applications*, vol. 7, 2018.

[10] P. K. Shukla, J. Kaur Sandhu, A. Ahirwar, D. Ghai, P. Maheshwary, and P. K. Shukla, "Multiobjective genetic algorithm and convolutional neural network based COVID-19 identification in chest X-ray images," *Mathematical Problems in Engineering*, vol. 2021, p. 9, 2021, https://doi.org/10.1155/2021/7804540, Article ID 7804540.

[11] A. Dey and K. N. Dey, "Automated glaucoma detection from fundus images of eye using statistical feature ex- traction methods and support vector machine classifica- tion," *Industry Interactive Innovations in Science, Engineering and Technology, Lecture Notes in Networks and Systems*, vol. 11, 2017.

[12] T. T. Htay and S. S. Maung, "Early stage breast cancer de-

tection system using GLCM feature extraction and K-nearest neighbor (k-NN) on mammography image," in *Proceedings of the 2018 18th International Symposium on Communications and Information Technologies (ISCIT)*, pp. 171–175, Bangkok, Thailand, 26-29 Sept. 2018.

[13] S. Pandit, P. K. Shukla, A. Tiwari, P. K. Shukla, and R. Dubey, "Review of video compression techniques based on fractal transform function and swarm intelligence," *International Journal of Modern Physics B*, vol. 34, no. 8, https://doi.org/10.1142/S0217979220500617, Article ID 2050061, 2020.

[14] Q. Abbas, "Glaucoma-deep: detection of glaucoma eye disease on retinal fundus images using deep learning," *International Journal of Advanced Computer Science and Applications*, vol. 7, January 2017.

[15] M. U. Muthmainah, H. A. Nugroho, and B. Winduratna, "Glaucoma classification based on texture and morphological features," in *Proceedings of the 2019 5th International Conference on Science and Technology (ICST)*, IEEE, Yogyakarta, Indonesia, 30-31 July 2019.

[16] S. Yu, D. Xiao, and Y. Kanagasingam, "Automatic detection of neovascularization on optic disk region with feature extrac- tion and support vector machine," in *Proceedings of the 201638th Annual International Conference of the IEEE Engineering in Medicine and Biology Society (EMBC)*, pp. 1324–1327, Orlando, FL, USA, 16-20 Aug. 2016.

[17] B. Li, Y. Chen, Y. Chen, Y. Lu, and C. Ma, "Landslide detection based on GLCM using SAR images," in *Proceedings of the IGARSS 2020 - 2020 IEEE International Geoscience and Remote Sensing Symposium*, pp. 1989–1992, Waikoloa, HI, USA, 26 Sept.-2 Oct. 2020.

[18] Y.-C. Tham, X. Li, T. Y. Wong, H. A. Quigley, T. Aung, and C.-Y. Cheng, "Global prevalence of glaucoma and projectionsof glaucoma burden through 2040," *Ophthalmology*, vol. 121, no. 11, pp. 2081–2090, 2014.

[19] A. Kesarwani, S. S. Chauhan, A. R. Nair, and G. Verma, "Supervised machine learning algorithms for fake news detection," in *Advances in Communication and Computational Technology. Lecture Notes in Electrical Engineering*, G. Hura, A. Singh, and L. Siong Hoe, Eds., vol. 668, Singapore, Springer, 2021.

[20] Z. Somogyi, "Performance evaluation of machine learning models," in *The Application of Artificial Intelligence*Springer, Cham, 2021.

[21] F. Bollwein and S. Westphal, "A branch & bound algorithm to determine optimal bivariate splits for oblique decision tree induction," *Applied Intelligence*, vol. 51, 2021.

[22] R. A. Utama, P. Sukarno, and E. M. Jadied, "Analysis and classification of danger level in android applications using naive Bayes algorithm," in *Proceedings of the 2018 6th International Conference on Information and Communication Technology (ICoICT)*, pp. 281–285, IEEE, Bandung, Indonesia, 3-5 May 2018.

[23] https://github.com/yiweichen04/retina_dataset/tree/master/dataset/2_glaucoma.

[24] T. S. Gill, B. A. Varghese, D. H. Hwang et al., "Juxtatumoral perinephric fat analysis in clear cell renal cell carcinoma," *Abdominal Radiology*, vol. 44, no. 4, pp. 1470–1480, 2019.

[25] J. Nalepa and M. Kawulok, "Selecting training sets for support vector machines: a review," *Artificial Intelligence Review*, Springer, vol. 52, no. 2, pp. 857–900, 2019.

[26] M. A. jabbar, B. L. Deekshatulu, and P. Chandra, "Classification of heart disease using K- nearest neighbor and genetic algorithm," *Procedia Technology*, vol. 10, pp. 85–94, 2013.

[27] IIT Hyderabad, Provided by Medical Image Processing (MIP) group., https://www.iith.ac.in/~lfovia/.

[28] J. B. Jonas, A. Bergua, P. Schmitz-Valckenberg, K. I. Papastathopoulos, and W. M. Budde, "Ranking of optic disc variables for detection of glaucomatous optic nerve damage," *Investigative Ophthalmology & Visual Science*, vol. 41, pp. 1764–1773, 2000.

[29] G. Khambra and P. Shukla, "Novel machine learning applications on fly ash based concrete: An overview," *Materials Today Proceedings*, vol. 7, pp. 2214–7853, 2021.

[30] Vejjanugraha, P., Kongprawechnon, W., Kondo, T., Tungpimolrut, K., Kotani, K. (2017). An automatic screening method for primary openangle glaucoma assessment using binary and multi-class support vector machines. ScienceAsia, 43(4), 229